Biological Journal of the Linnean Society, 2020, **129**, 14–25. With 3 figures.

Macroevolutionary trends of brain mass in Primates

M. MELCHIONNA[1], A. MONDANARO[1,2], C. SERIO[1], S. CASTIGLIONE[1], M. DI FEBBRARO[3], L. ROOK[2], J. A. F. DINIZ-FILHO[4], G. MANZI[5], A. PROFICO[5], G. SANSALONE[6] and P. RAIA[1*]

[1]*Dipartimento di Scienze della Terra, dell'Ambiente e delle Risorse, Università degli Studi di Napoli Federico II, Italy*
[2]*Department of Earth Sciences, University of Florence, Italy*
[3]*Dipartimento di Bioscienze e Territorio, University of Molise, C. da Fonte Lappone, 15, 86090 Pesche, IS, Italy*
[4]*Departamento de Ecologia, ICB, Universidade Federal de Goiás, Goiânia, GO, Brazil*
[5]*Department of Environmental Biology, Sapienza University of Rome, Italy*
[6]*Department of Environmental and Rural Sciences, FEARlab, University of New England, Armidale, 2351, NSW, Australia*

Received 31 July 2019; revised 16 September 2019; accepted for publication 17 September 2019

A distinctive trait in primate evolution is the expansion in brain mass. The potential drivers of this trend and how and whether encephalization influenced diversification dynamics in this group are hotly debated. We assembled a phylogeny accounting for 317 primate species, including both extant and extinct taxa, to identify macroevolutionary trends in brain mass evolution. Our findings show that Primates as a whole follow a macroevolutionary trend for an increase in body mass, relative brain mass and speciation rate over time. Although the trend for increased encephalization (brain mass) applies to all Primates, hominins stand out for their distinctly higher rates. Within hominins, this unique trend applies linearly over time and starts with *Australopithecus africanus*. The increases in both speciation rate and encephalization begin in the Oligocene, suggesting the two variables are causally associated. The substitution of early, stem Primates belonging to plesiadapiforms with crown Primates seems to be responsible for these macroevolutionary trends. However, our findings also suggest that cognitive capacities favoured speciation in hominins.

ADDITIONAL KEYWORDS: ECV – extinction rate – macroevolution – Primates – RRphylo – *search.trend* – speciation rate.

INTRODUCTION

The last common ancestor of primates lived some 71–63 Mya (Springer *et al.*, 2012). The oldest known stem Primates, the possibly polyphyletic plesiadapiforms, appeared in North America around the Palaeocene/Eocene boundary (Kay *et al.*, 1990; Bloch & Silcox, 2001; Bloch *et al.*, 2007). From the tiny, strictly arboreal pleasiadapiforms (Silcox *et al.*, 2017) to today's larger, ecologically versatile Strepsirhini and Haplorhini, primates have experienced evolution towards larger brains, in terms of both absolute brain volume and relative to body mass (Montgomery *et al.*, 2016). Such a high degree of encephalization is known to influence physiological, ecological and anatomical attributes in extant species (Gould, 1975; Deacon, 1990; Dunbar & Shultz, 2017; Neaux *et al.*, 2018). For instance, because brain tissue is some ten times more 'expensive' than any other tissue in the mammalian body, large-brained primate species have to subsist on high-quality food (Aiello & Wheeler, 1995; Mink *et al.*, 1981; Isler & van Schaik, 2006, 2009a). However, because developing a large brain is a costly and lengthy process, a number of life history traits, including sexual maturation (Barton & Capellini, 2011), slow down in large-brained species. From an anatomical perspective, evolving a large brain imposes constraints on skull shape variability (Mitteroecker & Bookstein, 2008; Profico *et al.*, 2017; Neaux *et al.*, 2018).

*Corresponding author. E-mail: pasquale.raia@unina.it

The large costs incurred by increased encephalization appear to be offset by either expanded cognitive abilities in social species (Kudo & Dunbar, 2001; Deaner *et al.*, 2007; Dunbar, 2009), enhanced capacities for psychological manipulation and female control in monogamous species (Schillaci, 2006), improved dexterity (Heldstab *et al.*, 2016), or better foraging abilities linked to frugivory (DeCasien *et al.*, 2017). However, it remains unclear whether social or ecological motives dominated the evolution of brain expansion in Primates (Powell *et al.*, 2017). In addition, the evolution of larger brains (in absolute terms) could also be a mere byproduct of a macroevolutionary trend for increased body mass. This ubiquitous pattern, known as Cope's rule (i.e. the evolutionary trend for phyletic lineages to increase in body mass over time; Cope, 1896; Soligo, 2006; Raia *et al.*, 2012), applies to plesiadapiforms, but not to Primates as a whole, although the latter are generally larger bodied than the former (Soligo, 2006). Still at the macroevolutionary level, a significant association between increased brain mass and speciation and extinction dynamics is often reported in the scientific literature (Lefebvre *et al.*, 2004; Nevo *et al.*, 2009; Isler & van Schaik, 2009b; Aristide *et al.*, 2016). Large brain mass correlates with low extinction risk in birds (Sol *et al.*, 2005) and mammals (Sol *et al.*, 2008; Isler & van Schaik, 2009b). A significant increase in brain mass is linked to a positive shift in diversification rate (i.e. increased difference between speciation and extinction rates) in carnivores (Finarelli & Flynn, 2009). Clade-level endocranial volume patterns are associated with origination and extinction in hominids (Du *et al.*, 2018). Other studies found an opposite (i.e. positive) relationship between increased brain mass and extinction risk in mammals (Abelson, 2016; Gonzalez-Voyer *et al.*, 2016) possibly mediated by the slow life history usually associated with having a large brain (Barton & Capellini, 2011). There is substantial evidence for an increase in speciation rates over time in Primates (Gómez & Verdú, 2012; Arbour & Santana, 2017; Herrera, 2017). Yet, how these rates relate to relative brain mass and to body mass remains unknown. Here, we hypothesized that Primates follow (1) a trend for increased body mass over time and (2) a trend for increased encephalization, and we tested (3) whether these trends are associated with each other and with diversification dynamics.

To test these hypotheses, we used a large palaeontological phylogeny comprising 317 primate species for which endocranial volumes and body mass estimates are available (Raia *et al.*, 2018). We applied Phylogenetic Ridge Regression (RRphylo, Castiglione *et al.*, 2018) to search for possible shifts in the evolutionary rate of encephalization across the Primates tree. We then assessed whether relative brain mass has increased over time, by applying a recently developed technique for testing macroevolutionary trends among and within clades (Castiglione *et al.*, 2019). Finally, we computed interval-to-interval speciation and extinction rates by applying an implementation of Pradel models on the palaeontological data. Per-interval rates were used to assess whether increased encephalization is associated with species diversification in Primates.

MATERIAL AND METHODS

Data preparation

We collected from the literature estimates of primate body mass and endocranial volume (ECV; see Supporting Information, Appendix S1). Our dataset and tree include 317 species, both extant (248) and extinct (69), ranging from Palaeogene plesiadapiforms to extinct and living primates.

Brain mass scales allometrically with body mass (Isler *et al.*, 2008; Grabowski *et al.*, 2016). Therefore, most studies addressing encephalization patterns have focused on the encephalization quotient (EQ, Jerison, 2012), usually calculated as the ratio between the observed and the allometrically predicted brain mass for a given body mass (Grabowski *et al.*, 2016; DeCasien *et al.*, 2017). However, both brain and body mass influence EQ. This complicates the identification of their relative impacts on encephalization, so that brain–body mass regression residuals are often used to represent the degree of encephalization as an alternative to EQs (Montgomery *et al.*, 2010; Shultz & Dunbar, 2010). Unfortunately, using residuals brings its own problems, because they have undesirable statistical properties if used in a phylogenetically explicit context (Freckleton, 2009). We therefore performed a multiple phylogenetic regression using ECV as the response variable, and phylogeny and body mass as the predictors. However, because the use of EQs has a long tradition in studies of encephalization, we additionally used EQ as the response variable, quantifying EQ as:

$$EQ = \frac{ECV}{e^{0.60 \ln(BM) - 1.402}} \quad (1)$$

where ECV is the endocranial volume and BM is body mass (Grabowski *et al.*, 2016).

We subsequently developed a third metric for encephalization (i.e. relative brain mass, RBM) which is the residual of the regression between (ln) ECV and (ln) body mass. It makes little sense to test for the effect of body mass variation on encephalization patterns if mass itself does not follow any trend. Therefore, we also tested for the existence of a trend in body mass (i.e. Cope's rule) as a preliminary analysis.

Phylogenetic multiple regression with RRphylo

We applied a recently implemented phylogenetic comparative method (PCM) that is specifically designed to process phylogenies including fossil species. The RRphylo method (developed in R software; Castiglione *et al.*, 2018) performs phylogenetic ridge regression (Kratsch & McHardy, 2014) to compute phenotypic evolutionary rates for each branch of the phylogeny and to estimate the ancestral phenotypes. Phylogenetic ridge regression consists of finding the maximum-likelihood solution to the problem of simultaneously estimating the regression coefficients, which describe the rate of phenotypic change from one node to the next for all branches of the tree. In this framework, the evolutionary rate coefficients are penalized to minimize the rate variation within clades (Castiglione *et al.*, 2018). Its advantage over traditional PCMs is that rates and ancestral state estimates are directly derived from the fossil data without assuming any a priori evolutionary model. We implemented multiple RRphylo regression (see Supporting Information, 'Multiple RRphylo, theory and testing') to calculate the phenotypic evolutionary rates and ancestral state estimates for each branch and node in the tree, respectively. For each response variable (i.e. body mass, ECV, RBM and EQ; results for EQ and RBM are presented in the Supporting Information) we searched for rate shifts across the tree by applying the function *search.shift* (Castiglione *et al.*, 2018). This function automatically scans the phylogeny to locate clades showing significantly higher/lower absolute phenotypic rate values than the rest of the tree. Significance is assessed through randomization. We tested for the existence of macroevolutionary trends in the phenotypes and rates by using the function *search.trend* (Castiglione *et al.*, 2019) in RRphylo. In *search.trend*, phenotypes and (absolute) evolutionary rate values are regressed against their distance from the tree root and the regression slopes compared to Brownian motion simulations to assess significance. In contrast to other phylogenetic comparative methods, *search.trend* allows us to compare different clades within the tree to each other in terms of the intensity (slope) of the macroevolutionary trend.

To assess for potential biases introduced by phylogenetic uncertainty, we applied the RRphylo function *overfitRR*. This function randomly removes a number of tips corresponding to 25% of the tree size and swaps a species' phylogenetic position (thereby accounting for sampling effects) by using the RRphylo function *swapONE*. Under *swapONE*, each tip might change its position on the tree by up to two nodes. For instance, a topology of the kind ((A,B),C) might change to ((C,B),A) or ((A,C),B). In addition, each node might change in age between the age of its ancestor and the age of its daughter node. We set one-tenth of the tips to be swapped across nodes and one-tenth of the nodes to be changed in age at each iteration. The function then performs *search.trend* and *search.shift* on the pruned tree and data. The procedure is repeated 100 times and the percentage of significant results returned. In this case, we specified the shifting clade to be tested for temporal trends in phenotypic (body mass) mean and rates.

The functions are available on CRAN (https://cran.r-project.org/web/packages/RRphylo/index.html). The multiple regression versions of *RRphylo* are available at https://github.com/pasraia/RRphylo.

Pradel models

Pradel models (Pradel, 1996) belong to the Jolly–Seber family of capture–mark–recapture (CMR) models. In keeping with Finarelli and Liow (Liow & Finarelli, 2014; Finarelli & Liow, 2016) we used this implementation on palaeontological data to estimate interval-to-interval extinction, origination, diversification and sampling probabilities. This method gives advantages over more traditional approaches. Foote (2000) developed the computation of instantaneous per-capita speciation and extinction rates, but excluded 'singleton taxa' (taxa confined to a specific time bin) to account for over-sampling. Alroy (2008) calculated an interval-specific sampling probability by taking into account the number of species that are present and sampled in three consecutive intervals and those sampled only in the first and last interval (and are thereby presumably missing because of sampling in the middle interval). With Pradel models absences are interpreted as either real absences or as failed-to-recognize presence. Hence, sampling probability is estimated jointly with the other parameters. For these reasons the method is recommended with palaeontological data, especially with heterogeneous and incomplete sampling (Liow & Finarelli, 2014).

Under Pradel models, survival probability (φ_i) is defined as the probability of a species surviving from interval i to interval $i + 1$. Thus, the complement of this term ($1 - \varphi_i$) is the probability of extinction from time i to time $i + 1$. Seniority (γ_i) is the probability that a species extant at interval i was already present during the interval $i - 1$. Thus, the complement of this term ($1 - \gamma_i$) is the speciation probability from time $i - 1$ to time i. This parameter is related to recruitment, f_i, which is the number of new species appearing at interval $i + 1$ divided by the number of species present at interval i. Recruitment is computed as: $f_i = \varphi_i \left(\frac{1-\gamma_{i+1}}{\gamma_{i+1}}\right)$. Growth rate ($\lambda_i$) is defined as the ratio between the number of species at intervals $i + 1$ and i. It can be also computed as: $\lambda_i = f_i + \varphi_i$. Therefore, the

net per-capita diversification rate is: $\frac{N_{i+1}-N_i}{N_i} = \lambda_i - 1$. Finally, sampling probability (p_i) is the probability of an extant species during interval i being sampled in that particular interval.

We split fossil occurrences in consecutive, 1-Myr time bins. We then built two types of Pradel models, one based on the estimation of 'survival and seniority' (which fits extinction, speciation and sampling rates) and the other on the estimation of 'survival and population growth' (which fits extinction, diversification and sampling rates) through time. The application of two different models is necessary because parameters are linear functions of each other (i.e. they are defined by a family of linear equations).

We were interested in the course of diversification metrics (speciation and extinction) over time, and how and whether they were affected by encephalization patterns. Therefore, we developed 12 different Pradel models overall (Table 1), where parameter estimates were a function of time, ECV and their combination. For each model, we implemented one version with constant sampling probability over time, and another version where sampling was allowed to change from one time bin to the next. The motivation was that sampling affects diversification metrics, and it is hard to tell whether sampling follows a random walk path or is highly variable among intervals (see Table 1 for the description of individual models). Model selection was based on corrected Akaike information criterion (AICc) values. Parameter estimates were finally derived through maximum-likelihood optimization.

RESULTS

Body mass

Results for body mass show an increase in average rates in *Colobus* + *Pliocolobus* + *Procolobus* monkeys, whereas Pitheciinae + Callibecinae and Indriidae show an opposite pattern (Table 2A). There is a general positive trend for body mass along the evolutionary history of Primates (Table 2B). More details on the trends in *Colobus* + *Pliocolobus* + *Procolobus*, Pitheciinae + Callibecinae and Indriidae, and on between-group comparisons are given in the Supporting Information (Tables S1 and S2). Because hominins (genus *Homo* plus australopiths and genus *Paranthropus*) are well known for their exceptional ECVs (see below) we eventually performed the same analysis focusing on the hominin node (Table S3).

ECV

We found significantly lower average rates of ECV increase in Hylobatidae, *Macaca*, the clade including *Cercopithecus* + *Erythrocebus* + *Chlorocebus* monkeys, Lorisoidea and *Saguinus* (Table 3, Fig. 1). Only hominins showed significantly higher average rates than the rest of the tree (Table 3).

Macroevolutionary trends in ECV and absolute rates of ECV for Primates as a whole are both significantly positive (Table 4A). In testing single clades, we found instances of significant temporal trends in ECV for all tested clades (Table 4B). There was a significantly higher temporal trend in ECV evolutionary rates for the hominin clade (Fig. 2). when compared to the rest of the tree (slope difference = 0.027, $P < 0.001$; Table 4C).

Table 1. Pradel models implemented in this study

Model	Survival (Phi)	Sampling (p)	Growth (Lambda)	Seniority (Gamma)
Phi(~time)p(~time)Gamma(~time)	time	time	–	time
Phi(~time)p(~time)Lambda(~time)	time	time	time	–
Phi(~1)p(~1)Gamma(~1)	constant	constant	–	constant
Phi(~1)p(~1)Lambda(~1)	constant	constant	constant	–
Phi(~1)p(~time)Gamma(~1)	constant	time	–	constant
Phi(~1)p(~time)Lambda(~1)	constant	time	constant	–
Phi(~ECV)p(~ECV)Gamma(~ECV)	ECV	ECV	–	ECV
Phi(~ECV)p(~ECV)Lambda(~ECV)	ECV	ECV	ECV	–
Phi(~time*ECV)p(~time*ECV)Gamma(~time*ECV)	time*ECV	time*ECV	–	time*ECV
Phi(~time*ECV)p(~time*ECV)Lambda(~time*ECV)	time*ECV	time*ECV	time*ECV	–
Phi(~ECV)p(~time*ECV)Gamma(~ECV)	ECV	time*ECV	–	ECV
Phi(~ECV)p(~time*ECV)Lambda(~ECV)	ECV	time*ECV	ECV	–

Column names indicate individual models (Model) and how survival (Phi), sampling probability (p), growth rate (Lambda) and seniority (Gamma) were fitted. Parameters were Survival (the complement to extinction risk), Sampling (the probability of a species being sampled in a given interval), Growth (the complement of diversification rate) and Seniority (the complement of speciation rate); time, the parameter is allowed to vary through time; constant, the parameter is constant through time; ECV, endocranial volume.

Table 2. Results for body mass

A. Evolutionary rate shift in body mass		
	Average rate difference	*P*
Colobus + *Pliocolobus* + *Procolobus*	0.419	0.018
Pitheciinae + Callibecinae	−0.490	0.001
Indriidae	−0.286	0.020
B. Temporal trends in Primate body mass		
	slope	*P*
Body mass	0.003	0.047
Body mass evolutionary rates	−0.003	0.060

A, clades showing significant shifts in body mass evolutionary rates. Average rate difference = difference in average rates between the focal clade and the rest of the tree; *P* = significance level for the difference as assessed by means of randomization. B, evolutionary trends through time for body mass in Primates. slope = regression slope; *P* = significance level assessed by contrasting the real slope to slopes derived from Brownian motion simulations.

Table 3. Clades showing significant shifts in endocranial volume evolutionary rates

	Average rate difference	*P*
Hominins	0.091	<0.001
Hylobatidae	−0.016	0.018
Macaca	−0.013	0.012
Cercopithecus + *Erythrocebus* + *Chlorocebus*	−0.014	0.003
Lorisoidea	−0.018	0.001
Saguinus	−0.022	<0.001

Average rate difference = difference in average rates between the focal clade and the rest of the tree; *P* = significance level for the difference as assessed by means of randomization.

Lorisoidea and the clade including *Cercopithecus*, *Erythrocebus* and *Chlorocebus* show significantly smaller marginal means than the other clades (Table 4C).

Phylogenetic uncertainty

In 100% of cases we found a positive and significant trend in ECV. A positive and significant trend in body mass was confirmed in 27% of cases. A significant rate shift in ECV was preserved in hominins (99% of cases) and Lorisoidea (89% of cases). For hominins, Hylobatidae, *Macaca*, *Cercopithecus* + *Erythrocebus* + *Chlorocebus*, Lorisoidea and *Saguinus* we found instances of positive and significant trends in ECV in at least 78% of cases (96% in hominins). The differences in estimated marginal means between single clades and the rest of the tree for ECV were preserved in almost 100% of cases only in Lorisoidea and *Saguinus*. We found negative temporal trends in single clades evolutionary rates of ECV in hominins (42% of cases), *Cercopithecus* + *Erythrocebus* + *Chlorocebus* (35% of cases), Lorisoidea (12% of cases) and *Saguinus* (5% of cases). Average rate differences in body mass are significant in at least 30% of cases for Indriidae and hominins, and in 2% of cases in *Colobus* + *Pliocolobus* + *Procolobus*. The complete table with full results can be found in the Supporting Information (Tables S8 and S9).

Pradel models

For both types ('survival and growth rate' and 'survival and seniority'), the best Pradel model is the one in which parameter estimates are a function of ECV and sampling is allowed to change from one temporal bin to the next (Table 5). As models for growth rate and seniority are very similar (ΔAICc = 1.268), we retrieved estimates for extinction (1 – survival) and speciation (1 – seniority) rates from the latter.

According to the best Pradel model, there is a relationship between extinction and speciation rates and ECV. We extracted regression coefficients from model results and computed extinction and speciation rates for each ECV value, and finally for each species (Fig. 3A). We found an increasing trend in speciation rate and a decrease in the extinction rate for ECV.

We also calculated the average rate values for each time interval (Fig. 3B). We found an increase in speciation rate and a corresponding decrease in extinction rate starting from the Early Oligocene. The distance between the curves increases at the beginning of the Miocene.

Because hominins are generally regarded as outliers (in terms of endocranial volumes) among Primates, we decided to repeat the previously described analyses pruning hominins (*Homo* plus australopiths and *Paranthropus*) from our dataset. According to the best Pradel model (Supporting Information, Table S10), the temporal and the phenotypic trends are confirmed even without hominins (Fig. S2). The *search.trend* analysis revealed a positive and significant trend in ECV for the whole tree (slope = 0.006, $P < 0.001$).

DISCUSSION

Here we have investigated the macroevolutionary patterns in primate body mass and encephalization. Primates follow Cope's rule (Cope, 1896; Soligo, 2006; Raia *et al.*, 2012) and show a clear trend for

Table 4. Evolutionary trends through time for endocranial volume (ECV), for Primates (A) and single Primate clades (B and C)

A. Temporal trends in Primate ECV

	Slope	*P*
ECV	0.006	<0.001
ECV evolutionary rates	0.006	<0.001

B. Temporal trends in single clades ECV

	Slope	*P*	Marginal means difference	*P* marginal means difference
Hominins	0.163	<0.001	0.121	<0.001
Hylobatidae	0.080	<0.001	0.048	0.000
Macaca	0.073	<0.001	0.018	0.032
Cercopithecus + *Erythrocebus* + *Chlorocebus*	0.046	<0.001	0.028	<0.001
Lorisoidea	0.004	<0.001	−0.002	0.807
Saguinus	0.037	<0.001	−0.006	0.633

C. Temporal trend in single clades ECV evolutionary rates

	Marginal means difference	*P* marginal means difference	Slope difference	*P* slope difference
Hominins	0.090	0.000	0.027	<0.001
Hylobatidae	−0.017	0.123	0.001	0.893
Macaca	−0.015	0.057	0.003	0.357
Cercopithecus + *Erythrocebus* + *Chlorocebus*	−0.016	0.032	0.003	0.238
Lorisoidea	−0.018	0.045	0.000	0.952
Saguinus	−0.021	0.047	−0.001	0.833

Slope = regression slope; *P* = significance level assessed by contrasting the real slope to slopes derived from Brownian motion simulations; *P* marginal means difference = *P* value for the difference in marginal means contrasting single Primate clades to all other Primates; slope difference = the difference between regression slopes for single clades contrasted to the slope obtained for all other Primates; *P* slope difference = *P* for the difference in slopes between single clades and the other Primates.

Table 5. Results for comparison of Pradel models

Model	npar	AICc	ΔAICc	Weight	Deviance
Phi(~ECV)p(~time * ECV)Lambda(~ECV)	130	1385.277	0	0.653	1012.495
Phi(~ECV)p(~time * ECV)Gamma(~ECV)	130	1386.544	1.268	0.347	1013.763
Phi(~1)p(~time)Lambda(~1)	65	1470.945	85.668	0	519.581
Phi(~1)p(~time)Gamma(~1)	65	1471.476	86.199	0	520.111
Phi(~time)p(~time)Gamma(~time)	187	1603.661	218.384	0	144.687
Phi(~ECV)p(~ECV)Lambda(~ECV)	6	1714.860	329.584	0	1702.663
Phi(~ECV)p(~ECV)Gamma(~ECV)	6	1722.162	336.885	0	1709.965
Phi(~1)p(~1)Gamma(~1)	3	1923.963	538.686	0	1119.922
Phi(~1)p(~1)Lambda(~1)	3	1923.963	538.686	0	1119.922
Phi(~time * ECV)p(~time * ECV)Gamma(~time * ECV)	374	6239.486	4854.209	0	655.279
Phi(~ECV)p(~time * ECV)Lambda(~ECV)	130	1385.277	0	0.653	1012.495

npar = number of parameters; AICc = corrected Akaike information criterion; ΔAICc = the difference in the AIC value between each model and the model with the lowest AIC; weight = normalized Akaike weights; deviance = model deviance.

increased ECV over time. Nonetheless, hominins have unambiguously larger ECVs (as well as larger RBM and EQ values) than other primates and show a significantly stronger tendency for increased encephalization over time than any other primate clade (Fig. 1).

During their evolutionary history, Primates experienced trends for (1) larger body mass, (2) increased encephalization (in keeping with our first hypothesis), (3) lower extinction rate and (4) higher speciation rate, and (5) hominins stand out for their exceptionally large brain and more intense encephalization pattern. Cope's rule does not produce the observed encephalization pattern. Although both body and brain mass increased through time in the Primate clade, relative encephalization itself increased, meaning that the primate brain became proportionally larger. This trend became evident with the appearance of crown Primates and is associated with an increased speciation rate in this clade, starting during the Oligocene.

The macroevolutionary pattern towards larger brain mass is not driven by the disproportionately large ECVs typical of hominins, indicating that the connection between higher speciation rates and larger ECV is a defining aspect of the evolutionary history of crown Primates. An increase in encephalization has been repeatedly proposed as promoting diversification in birds (Sol *et al.*, 2005), mammals (Sol *et al.*, 2008) and hominins (Du *et al.*, 2018; González-Forero & Gardner, 2018), although it has been strongly questioned elsewhere (Abelson, 2016; Gonzalez-Voyer *et al.*, 2016). Larger relative brain mass is said to favour behavioural plasticity, adaptation to variable environmental conditions and ecological reliance (Sol *et al.*, 2008). However, mammals with large brains usually have small litter size, longer gestation time and older age at sexual maturation (Barton & Capellini, 2011), potentially exposing them to greater extinction risk. These findings make it difficult to determine whether the relationship between brain mass and speciation trends is more than accidental. Unfortunately, we had to calculate speciation rates interval by interval, and the trend in ECV as continuous. This means that we cannot comment on the apparent relationship between the two variables beyond their pure association.

Although the finding that hominins have exceedingly large brains is not novel, it is intriguing that australopiths (since the appearance of *A. africanus*) and *Homo* share a rapid evolution of high ECV values and remain significantly different from any other Primate clade with regard to several additional aspects, including tool use (Skinner *et al.*, 2015), full bipedalism (Dowdeswell *et al.*, 2017) and mandible evolutionary rates (Raia *et al.*, 2018). The evolution of a larger brain in hominins is usually discussed as a gradual process punctuated by stepwise encephalization pulses (Du *et al.*, 2018; Diniz-Filho *et al.*, 2019). In agreement with this scenario, we found that hominins, as a whole, represent an instance of positive rate shift in ECV among Primates, yet within this lineage the progressive encephalization appears to be a gradual process starting around the appearance of *A. africanus* (Dart, 1925) (Fig. 2). Falk *et al.* (2000) recognized *A. africanus* as showing a distinct brain shape (rather than brain mass) as compared to *Paranthropus*, suggesting that a shift in the arrangement of brain cortical areas took place within hominins starting with *A. africanus*.

Looking at Primates as a whole, our results show that the positive relationship between ECV and speciation rates becomes evident from the early Oligocene (Fig. 3B). The Oligocene marked a period of intense climatic change

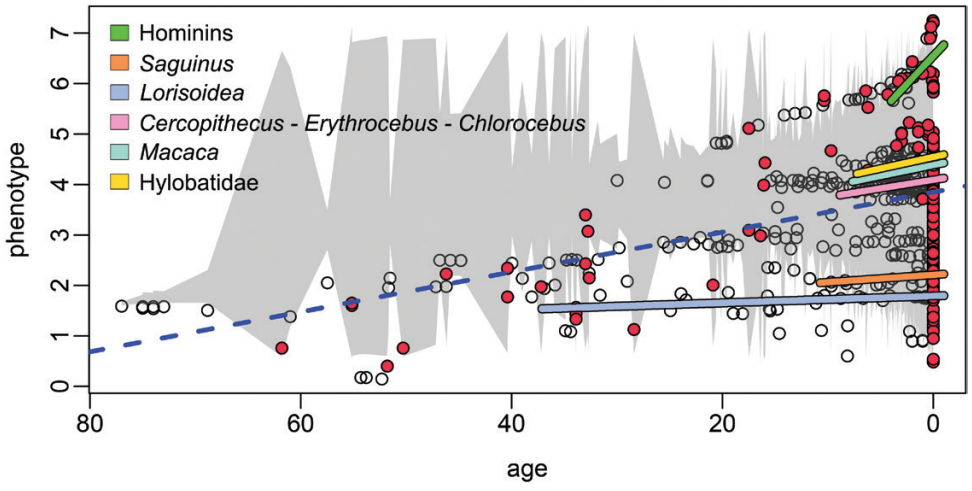

Figure 1. Macroevolutionary patterns in endocranial volume. Red circles represent actual phenotypes, while open circles represent ancestral state estimates as produced by RRphylo. The y-axis represents the natural logarithm of the endocranial volume, in cubic centimeters. The x-axis represents time before present, in million years.

and major turnover in the history of mammals in general, and primates in particular (Prothero, 2012). The global climatic cooling near the Eocene–Oligocene boundary (Zachos *et al.*, 2001) was the major driver of such intense species turnover, and of a major peak in the extinction rate curve. Thereafter, there was an increase in diversification

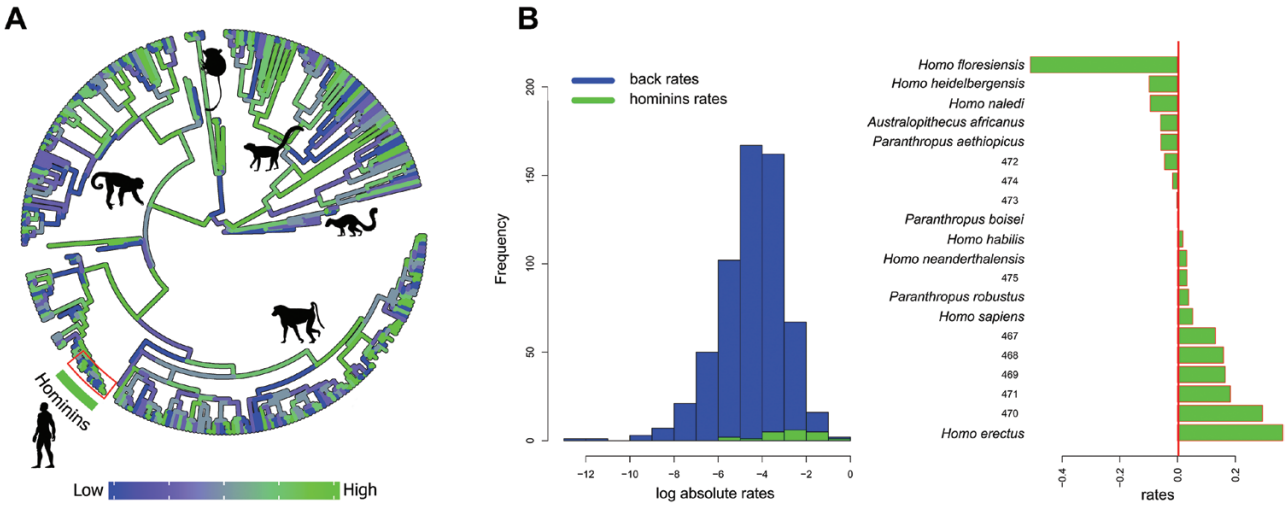

Figure 2. A, Primate phylogeny. The colour gradient associated with the branches represents estimated rates of endocranial volume evolution. B, absolute rates of individual branches of the hominin clade collated in increasing rate value (green bars), and contrasted with the average rate computed over the rest of the tree branches (vertical red line). Bars without names correspond to internal nodes. The image was generated by using the R package ggplot (http://ggplot2.org/) and our own R codes. Animal silhouettes were available under Public Domain licence at phylopic (http://phylopic.org/), unless otherwise indicated. Specifically, *Homo sapiens* (http://phylopic.org/image/c089caae-43ef-4e4ebf26-973dd4cb65c5/); *Cebus* (http://phylopic.org/image/156b515d-f25c-4497-b15b-5afb832cc70c/), available for reuse under the Creative Commons Attribution 3.0 Unported (https://creativecommons.org/licenses/by/3.0/) image by Sarah Werning; *Tarsius* (http://phylopic.org/image/f598fb39-facf-43ea-a576-1861304b2fe4/); lemuriformes (http://phylopic.org/image/eefe8b60-9a26-46ed-a144-67f4ac885267/), available for reuse under Attribution-ShareAlike 3.0 Unported (https://creativecommons.org/licenses/by-sa/3.0/) image by Smokeybjb; *Plesiadapis* (http://phylopic.org/image/b6ff5568-0712-4b15-a1fd-22b289af904d/), available for reuse under Attribution-ShareAlike 3.0 Unported (https://creativecommons.org/licenses/by-sa/3.0/) image by Nobu Tamura (modified by Michael Keesey).

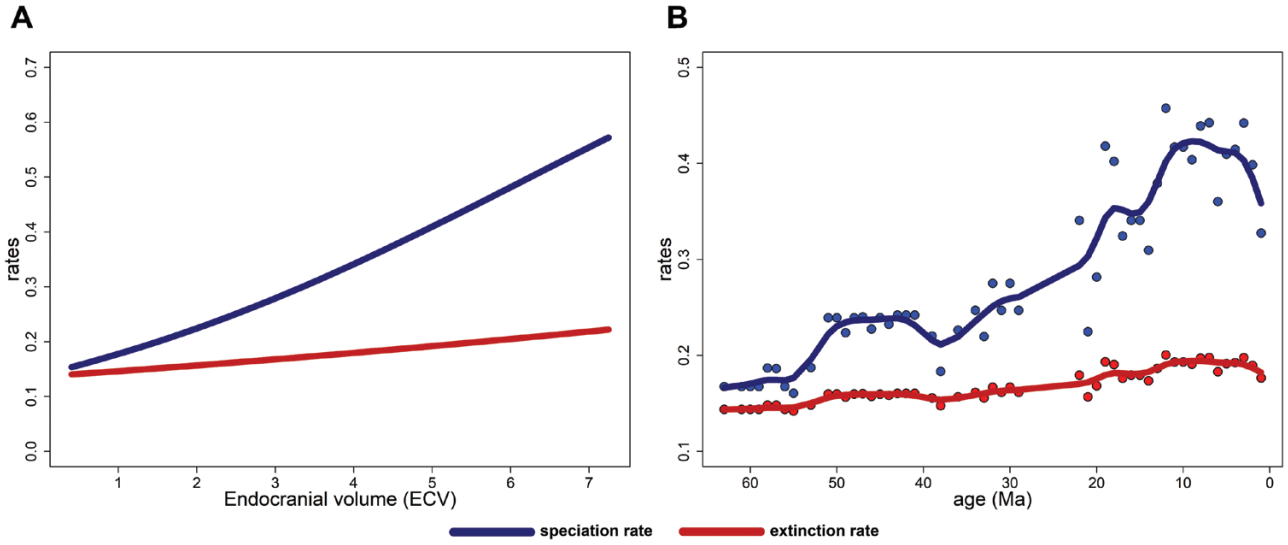

Figure 3. A, statistical relationship between speciation and extinction rates and endocranial volume. B, patterns of speciation and extinction rates plotted against time.

rates in Primates (Arbour & Santana, 2017; Herrera, 2017). This is consistent with our conclusions, which point to a peak in speciation rate during the Miocene (Fig. 3B), and with genetic analyses linking the intense Miocene primate diversification to higher global mean temperatures (Springer *et al.*, 2012).

We did not explicitly test for a possible role of feeding ecology or mating system on brain mass. DeCasien *et al.* (2017) showed that frugivorous primates exhibit larger brains than folivore species, in association with or possibly as a consequence of their highly manipulative mode of foraging. Our data show that a significant shift in ECV evolutionary rates and larger than expected (by phylogenetic position) brain mass only pertain to hominins. Conversely, instances of decreased evolutionary rates in ECV pertain to both folivorous and frugivorous clades (Tables 3 and 4). Categorizing primate diets is difficult, because of seasonal and geographical variation in feeding habits even within the same species. Hence, this important issue remains to be elucidated. Several reports have linked larger brains with polygamous mating systems (Shultz & Dunbar, 2007) or quite the opposite (Schillaci, 2006). As per diet, we did not directly investigate the relationship between brain mass evolution and social system, because of the obvious difficulty of assessing the degree of sociality in extinct species. However, it is of note that within hominins at least, both monogamous and polygamous species are included, suggesting that the effect of sociality deserves further investigation as well.

This study demonstrates that increased encephalization is a macroevolutionary pattern defining the primates as a group, and hominins in particular. The increase in ECV (as well as RBM and EQ) and speciation rates coincided with the appearance of Anthropoidea and accelerated significantly within hominins.

ACKNOWLEDGEMENTS

We are grateful to Fabio Di Vincenzo and Francesco Carotenuto for comments and exchange of ideas on earlier versions of the manuscript. We also thank two anonymous reviewers for their helpful comments. The authors declare no conflicts of interest.

REFERENCES

Abelson ES. 2016. Brain size is correlated with endangerment status in mammals. *Proceedings of the Royal Society B: Biological Sciences* **283:** 20152772.

Aiello LC, **Wheeler P. 1995.** The expensive-tissue hypothesis: the brain and the digestive system in human and primate evolution. *Current Anthropology* **36:** 199–221.

Alroy J. 2008. Colloquium paper: Dynamics of origination and extinction in the marine fossil record. *Proceedings of the National Academy of Sciences of the United States of America* **105**(Suppl 1): 11536–11542.

Arbour JH, **Santana SE. 2017.** A major shift in diversification rate helps explain macroevolutionary patterns in primate species diversity. *Evolution* **71:** 1600–1613.

Aristide L, **dos Reis SF**, **Machado AC**, **Lima I**, **Lopes RT**, **Perez SI. 2016.** Brain shape convergence in the adaptive radiation of New World monkeys. *Proceedings of the National Academy of Sciences of the United States of America* **113:** 2158–2163.

Barton RA, **Capellini I. 2011.** Maternal investment, life histories, and the costs of brain growth in mammals. *Proceedings of the National Academy of Sciences of the United States of America* **108:** 6169–6174.

Bloch JI, **Silcox MT. 2001.** New basicrania of Paleocene-Eocene *Ignacius*: re-evaluation of the Plesiadapiform–Dermopteran link. *American Journal of Physical Anthropology* **116:** 184–198.

Bloch JI, **Silcox MT**, **Boyer DM**, **Sargis EJ. 2007.** New Paleocene skeletons and the relationship of plesiadapiforms to crown-clade primates. *Proceedings of the National Academy of Sciences of the United States of America* **104:** 1159–1164.

Castiglione S, **Serio C**, **Mondanaro A**, **Di Febbraro M**, **Profico A**, **Girardi G**, **Raia P. 2019.** Simultaneous detection of macroevolutionary patterns in phenotypic means and rate of change with and within phylogenetic trees including extinct species. *PLoS ONE* **14:** e0210101.

Castiglione S, **Tesone G**, **Piccolo M**, **Melchionna M**, **Mondanaro A**, **Serio C**, **Di Febbraro M**, **Raia P. 2018.** A new method for testing evolutionary rate variation and shifts in phenotypic evolution. *Methods in Ecology and Evolution* **62:** 181–10.

Cope E. 1896. *The primary factors of organic evolution*. Chicago: Open Court Publishing Company.

Deacon TW. 1990. Fallacies of progression in theories of brain-size evolution. *International Journal of Primatology* **11:** 193–236.

Deaner RO, **Isler K**, **Burkart J**, **van Schaik C. 2007.** Overall brain size, and not encephalization quotient, best predicts cognitive ability across non-human primates. *Brain, Behavior and Evolution* **70:** 115–124.

DeCasien AR, **Williams SA**, **Higham JP. 2017.** Primate brain size is predicted by diet but not sociality. *Nature Ecology & Evolution* **1:** 0112.

Diniz-Filho JAF, **Jardim L**, **Mondanaro A**, **Raia P. 2019.** Multiple components of phylogenetic non-stationarity in the evolution of brain size in fossil hominins. *Evolutionary Biology* **46:** 47–59.

Dowdeswell MR, **Jashashvili T**, **Patel BA**, **Lebrun R**, **Susman RL**, **Lordkipanidze D**, **Carlson KJ. 2017.** Adaptation to bipedal gait and fifth metatarsal structural

properties in *Australopithecus*, *Paranthropus*, and *Homo*. *Comptes Rendus Palevol* **16:** 585–599.

Du A, Zipkin AM, Hatala KG, Renner E, Baker JL, Bianchi S, Bernal KH, Wood BA. 2018. Pattern and process in hominin brain size evolution are scale-dependent. *Proceedings of the Royal Society B: Biological Sciences* **285:** 20172738.

Dunbar RIM. 2009. The social brain hypothesis and its implications for social evolution. *Annals of Human Biology* **36:** 562–572.

Dunbar RIM, Shultz S. 2017. Why are there so many explanations for primate brain evolution? *Philosophical Transactions of the Royal Society* **372:** 20160244.

Falk D, Redmond JC Jr, Guyer J, Conroy C, Recheis W, Weber GW, Seidler H. 2000. Early hominid brain evolution: a new look at old endocasts. *Journal of Human Evolution* **38:** 695–717.

Finarelli JA, Flynn JJ. 2009. Brain-size evolution and sociality in Carnivora. *Proceedings of the National Academy of Sciences of the United States of America* **106:** 9345–9349.

Finarelli JA, Liow LH. 2016. Diversification histories for North American and Eurasian carnivorans. *Biological Journal of the Linnean Society* **118:** 26–38.

Foote M. 2000. Origination and extinction components of taxonomic diversity. *Paleobiology* **26:** 74–102.

Freckleton RP. 2009. The seven deadly sins of comparative analysis. *Journal of Evolutionary Biology* **22:** 1367–1375.

Gómez JM, Verdú M. 2012. Mutualism with plants drives primate diversification. *Systematic Biology* **61:** 567–577.

González-Forero M, Gardner A. 2018. Inference of ecological and social drivers of human brain-size evolution. *Nature* **557:** 554–557.

Gonzalez-Voyer A, González-Suárez M, Vilà C, Revilla E. 2016. Larger brain size indirectly increases vulnerability to extinction in mammals. *Evolution* **70:** 1364–1375.

Gould SJ. 1975. Allometry in primates, with emphasis on scaling and the evolution of the brain. *Contributions to Primatology* **5:** 244–292.

Grabowski M. 2016. Bigger brains led to bigger bodies?: the correlated evolution of human brain and body size. *Current Anthropology* **57:** 174–196.

Grabowski M, Voje KL, Hansen TF. 2016. Evolutionary modeling and correcting for observation error support a 3/5 brain-body allometry for primates. *Journal of Human Evolution* **94:** 106–116.

Heldstab SA, Kosonen ZK, Koski SE, Burkart JM, van Schaik CP, Isler K. 2016. Manipulation complexity in primates coevolved with brain size and terrestriality. *Scientific Reports* **6:** 24528.

Herrera JP. 2017. Primate diversification inferred from phylogenies and fossils. *Evolution* **71:** 2845–2857.

Isler K, Christopher Kirk E, Miller JM, Albrecht GA, Gelvin BR, Martin RD. 2008. Endocranial volumes of primate species: scaling analyses using a comprehensive and reliable data set. *Journal of Human Evolution* **55:** 967–978.

Isler K, van Schaik CP. 2006. Metabolic costs of brain size evolution. *Biology Letters* **2:** 557–560.

Isler K, van Schaik CP. 2009a. The expensive brain: a framework for explaining evolutionary changes in brain size. *Journal of Human Evolution* **57:** 392–400.

Isler K, Van Schaik CP. 2009b. Why are there so few smart mammals (but so many smart birds)? *Biology Letters* **5:** 125–129.

Jerison H. 2012. *Evolution of the brain and intelligence*. Amsterdam: Elsevier.

Kay RF, Thorington RW, Houde P. 1990. Eocene plesiadapiform shows affinities with flying lemurs not primates. *Nature* **345:** 342–344.

Kratsch C, McHardy AC. 2014. RidgeRace: ridge regression for continuous ancestral character estimation on phylogenetic trees. *Bioinformatics* **30:** i527–i533.

Kudo H, Dunbar RIM. 2001. Neocortex size and social network size in primates. *Animal Behaviour* **62:** 711–722.

Lefebvre L, Reader SM, Sol D. 2004. Brains, innovations and evolution in birds and primates. *Brain, Behavior and Evolution* **63:** 233–246.

Liow LH, Finarelli JA. 2014. A dynamic global equilibrium in carnivoran diversification over 20 million years. *Proceedings of the Royal Society B: Biological Sciences* **281:** 20132312.

Mink JW, Blumenschine RJ, Adams DB. 1981. Ratio of central nervous system to body metabolism in vertebrates: its constancy and functional basis. *The American Journal of Physiology* **241:** R203–R212.

Mitteroecker P, Bookstein F. 2008. The evolutionary role of modularity and integration in the hominoid cranium. *Evolution* **62:** 943–958.

Montgomery SH, Capellini I, Barton RA, Mundy NI. 2010. Reconstructing the ups and downs of primate brain evolution: implications for adaptive hypotheses and *Homo floresiensis*. *BMC Biology* **8:** 9.

Montgomery SH, Mundy NI, Barton RA. 2016. Brain evolution and development: adaptation, allometry and constraint. *Proceedings of the Royal Society B: Biological Sciences* **283:** 20160433.

Neaux D, Sansalone G, Ledogar JA, Heins Ledogar S, Luk THY, Wroe S. 2018. Basicranium and face: assessing the impact of morphological integration on primate evolution. *Journal of Human Evolution* **118:** 43–55.

Nevo E, Pirlot P, Beiles A. 2009. Brain size diversity in adaptation and speciation of subterranean mole rats. *Journal of Zoological Systematics and Evolutionary Research* **26:** 467–479.

Powell LE, Isler K, Barton RA. 2017. Re-evaluating the link between brain size and behavioural ecology in primates. *Proceedings of the Royal Society B: Biological Sciences* **284:** 20171765–20171768.

Pradel R. 1996. Utilization of capture-mark-recapture for the study of recruitment and population growth rate. *Biometrics* **52:** 703.

Profico A, Piras P, Buzi C, Di Vincenzo F, Lattarini F, Melchionna M, Veneziano A, Raia P, Manzi G. 2017. The evolution of cranial base and face in Cercopithecoidea and Hominoidea: modularity and morphological integration. *American Journal of Primatology* **79:** e22721.

Prothero D. 2012. Cenozoic mammals and climate change: the contrast between coarse-scale versus high-resolution studies explained by species sorting. *Geosciences* **2:** 25–41.

Raia P, **Boggioni M**, **Carotenuto F**, **Castiglione S**, **Di Febbraro M**, **Di Vincenzo F**, **Melchionna M**, **Mondanaro A**, **Papini A**, **Profico A**, **Serio C**, **Veneziano A**, **Vero VA**, **Rook L**, **Meloro C**, **Manzi G. 2018.** Unexpectedly rapid evolution of mandibular shape in hominins. *Scientific Reports* **8:** 7340.

Raia P, **Carotenuto F**, **Passaro F**, **Fulgione D**, **Fortelius M. 2012.** Ecological specialization in fossil mammals explains Cope's rule. *The American Naturalist* **179:** 328–337.

Schillaci MA. 2006. Sexual selection and the evolution of brain size in primates. *PLoS ONE* **1:** e62.

Shultz S, **Dunbar R. 2010.** Encephalization is not a universal macroevolutionary phenomenon in mammals but is associated with sociality. *Proceedings of the National Academy of Sciences of the United States of America* **107:** 21582–21586.

Shultz S, **Dunbar RI. 2007.** The evolution of the social brain: anthropoid primates contrast with other vertebrates. *Proceedings of the Royal Society B: Biological Sciences* **274:** 2429–2436.

Silcox MT, **Bloch JI**, **Boyer DM**, **Chester SGB**, **López-Torres S. 2017.** The evolutionary radiation of plesiadapiforms. *Evolutionary Anthropology* **26:** 74–94.

Skinner MM, **Stephens NB**, **Tsegai ZJ**, **Foote AC**, **Nguyen NH**, **Gross T**, **Pahr DH**, **Hublin JJ**, **Kivell TL. 2015.** Human evolution. Human-like hand use in *Australopithecus africanus*. *Science (New York, N.Y.)* **347:** 395–399.

Sol D, **Bacher S**, **Reader SM**, **Lefebvre L. 2008.** Brain size predicts the success of mammal species introduced into novel environments. *The American Naturalist* **172**(Suppl 1): S63–S71.

Sol D, **Duncan RP**, **Blackburn TM**, **Cassey P**, **Lefebvre L. 2005.** Big brains, enhanced cognition, and response of birds to novel environments. *Proceedings of the National Academy of Sciences of the United States of America* **102:** 5460–5465.

Soligo C. 2006. Correlates of body mass evolution in primates. *American Journal of Physical Anthropology* **130:** 283–293.

Springer MS, **Meredith RW**, **Gatesy J**, **Emerling CA**, **Park J**, **Rabosky DL**, **Stadler T**, **Steiner C**, **Ryder OA**, **Janečka JE**, **Fisher CA**, **Murphy WJ. 2012.** Macroevolutionary dynamics and historical biogeography of primate diversification inferred from a species supermatrix. *PLoS ONE* **7:** e49521.

Zachos J, **Pagani M**, **Sloan L**, **Thomas E**, **Billups K. 2001.** Trends, rhythms, and aberrations in global climate 65 Ma to present. *Science* **292:** 686–693.

SUPPORTING INFORMATION

Additional Supporting Information may be found in the online version of this article at the publisher's website.

Figure S1. Sampling probability (p) estimation for the primate fossil record during the last 65 Myr.

Figure S2. Left: the statistical relationship between speciation and extinction rates and endocranial volume (ECV). Right: patterns of speciation and extinction rates plotted against time.

Table S1. Evolutionary trends through time for body mass in single Primate clades. Slope = regression slope; P = significance level assessed by contrasting the real slope to slopes derived from Brownian motion simulations; P marginal means difference = P for the difference in marginal means contrasting single Primate clades to all other Primates; slope difference = the difference between regression slopes for single clades contrasted to the slope obtained for all other Primates; P slope difference = P value for the difference in slopes between single clades and the other Primates.

Table S2. Group comparisons for body mass per group showing distinct evolutionary rates. Slope = regression slope; P = significance level assessed by contrasting the real slope to slopes derived from Brownian motion simulations; P marginal means difference = P value for the difference in marginal means contrasting single Primate clades to all other Primates; slope difference = the difference between regression slopes for single clades in contrast to the slope obtained for all other Primates; P slope difference = P value for the difference in slopes between single clades and the other Primates.

Table S3. Evolutionary trends through time for body mass in the hominin clade. Slope = regression slope; P = significance level assessed by contrasting the real slope to slopes derived from Brownian motion simulations; P marginal means difference = P value for the difference in marginal means contrasting the hominin clade to all other Primates; slope difference = the difference between regression slopes for the hominin clade contrasted to the slope obtained for all other Primates; P slope difference = P value for the difference in slopes between the hominin clade and the other Primates.

Table S4. Hominins clade showing significant shifts in RBM evolutionary rates. Average rate difference = difference in average rates between the focal clade and the rest of the tree; P = significance level for the difference as assessed by randomization.

Table S5. Evolutionary trends through time for RBM, for Primates (A) and hominins clade (B, C). Slope = regression slope; P = significance level assessed by contrasting the real slope to slopes derived from Brownian motion

simulations; *P* marginal means difference = *P* value for the difference in marginal means contrasting the hominin clade to all other Primates; slope difference = the difference between regression slopes for the hominin clade in contrast to the slope obtained for all other Primates; *P* slope difference = *P* value for the difference in slopes between the hominin clade and the other Primates.

Table S6. Hominin clade showing significant shifts in EQ evolutionary rates. Average rate difference = difference in average rates between the focal clade and the rest of the tree; *P* = significance level for the difference as assessed by randomization.

Table S7. Evolutionary trends through time for EQ, for Primates (A) and the hominin clade (B, C). Slope = regression slope; *P* = significance level assessed by contrasting the real slope to slopes derived from Brownian motion simulations; *P* marginal means difference = *P* value for the difference in marginal means contrasting the hominin clade to all other Primates; slope difference = the difference between regression slopes for the hominin clade in contrast to the slope obtained for all other Primates; *P* slope difference = *P* value for the difference in slopes between the hominin clade and the other Primates.

Table S8. Assessment of sampling and phylogenetic uncertainty. For each phenotype (first column) we counted the number of times either a positive (*P* slope+) of negative (*P* slope-) trend through time applies to the Primate tree by altering its topology and randomly sampling 75% of the original species only.

Table S9. Assessment of sampling and phylogenetic uncertainty. For each phenotype and individual clade (first column) we counted the number of times either a positive (*P* slope+) of negative (*P* slope-) trend through time applies to the Primate tree by altering its topology and randomly sampling 75% of the original species only.

Table S10. Results for comparison of Pradel models applied on the dataset after excluding hominins. npar = number of parameters; AICc = corrected Akaike information criterion; DeltaAICc = the difference in the AIC value between each model and the model with the lowest AIC; weight = normalized Akaike weights; Deviance = model deviance.

Table S11. Percentage of Type I and Type II errors for multiple- and simple *search.trend*. Trend in phenotype: temporal trend in phenotypic mean; trend in rates: temporal trend in evolutionary rates.